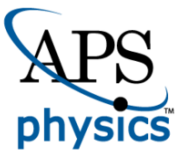

Gate-Efficient Simulation of Molecular Eigenstates on a Quantum Computer

M. Ganzhorn, D.J. Egger, P. Barkoutsos, P. Ollitrault, G. Salis, N. Moll, M. Roth, A. Fuhrer, P. Mueller, S. Woerner, I. Tavernelli, and S. Filipp

Phys. Rev. Applied **11**, 044092 — Published 30 April 2019

DOI: 10.1103/PhysRevApplied.11.044092

Gate-efficient simulation of molecular eigenstates on a quantum computer

M. Ganzhorn,[1] D.J. Egger,[1] P. Barkoutsos,[1] P. Ollitrault,[1] G. Salis,[1] N. Moll,[1]
M. Roth,[2,3] A. Fuhrer,[1] P. Mueller,[1] S. Woerner,[1] I. Tavernelli,[1] and S. Filipp[1]

[1] *IBM Research Zurich, Säumerstrasse 4, 8803 Rüschlikon, Switzerland*
[2] *JARA Institute for Quantum Information (PGI-11), Forschungszentrum Jülich, 52428 Jülich, Germany*
[3] *Institute for Quantum Information, RWTH Aachen University, 52056 Aachen, Germany*

(Dated: April 8, 2019)

A key requirement to perform simulations of large quantum systems on near-term quantum hardware is the design of quantum algorithms with short circuit depth that finish within the available coherence time. A way to stay within the limits of coherence is to reduce the number of gates by implementing a gate set that matches the requirements of the specific algorithm of interest directly in hardware. Here, we show that exchange-type gates are a promising choice for simulating molecular eigenstates on near-term quantum devices since these gates preserve the number of excitations in the system. We report on the experimental implementation of a variational algorithm on a superconducting qubit platform to compute the eigenstate energies of molecular hydrogen. We utilize a parametrically driven tunable coupler to realize exchange-type gates that are configurable in amplitude and phase on two fixed-frequency superconducting qubits. With gate fidelities around 95% we are able to compute the eigenstates within an accuracy of 50 mHartree on average, a limit set by the coherence time of the tunable coupler.

I. INTRODUCTION

The simulation of the electronic structure of molecular and condensed matter systems is a challenging computational task as the cost of resources increases exponentially with the number of electrons when accurate solutions are required. With the tremendous improvements in the control of complex quantum systems this bottleneck may be overcome by the use of quantum computing hardware [1]. Various algorithms for quantum simulation have been designed to that end, including adiabatic and quantum phase estimation algorithms [2, 3]. With these algorithms the challenges for practical applications lie in the efficient mapping of the electronic Hamiltonian onto the quantum computer and in the required number of quantum gates, respectively, that remains prohibitive on current and near-term quantum hardware [4] without quantum error correction schemes [5]. On the other hand, variational quantum eigensolver (VQE) methods [6, 7] can produce accurate results with a small number of gates [8] using algorithms with low circuit depth [9] and do not require a direct mapping of the electronic Hamiltonian onto the hardware. Moreover, such algorithms are inherently robust against certain errors [8, 10, 11] and are therefore considered as ideal candidates for first practical implementations on noisy intermediate scale quantum hardware.

Recently, the molecular ground state energy of hydrogen and helium have been computed via VQE in proof of concept experiments using NMR quantum simulators [12–14], photonic architectures [6] or nitrogen-vacancy centers in diamond [15]. Although very accurate energy estimates are obtained, quantum simulation of larger systems remains an intractable problem on these platforms because of the difficulties arising in scaling them up to more than a few qubits. For this reason trapped ions [16–19] and superconducting qubits [20–22] have become promising candidates to carry out VQE-based quantum simulations in particular for quantum chemistry applications. For instance, the ground state energies of molecules like H_2 [23–25], LiH and BeH_2 [24], as well as the energy spectrum of the four eigenstates of H_2 [25], have been measured on general purpose superconducting qubit platforms. In these experiments, a heuristic approach based on gates naturally available in hardware, such as C-Phase, CNOT or bSWAP, is employed. However, computing larger molecules with more orbitals in the active computational space becomes impractical with this method. Without further constraints, the dimension of the Hilbert space accessed via the parameterized gate sequences grows exponentially with the number of required qubits N. The probability to reach the wanted ground state decreases accordingly. It is, thus, important to use a set of entangling gates that matches the specifics of the problem [8]. For quantum chemistry calculation, each qubit typically represents the population of an electronic orbital [26, 27]. Since the number of electrons n_e is constant for a given molecular system or a chemical reaction, the number of qubit excitations is too. Qubit gates which preserve the number of excitations on the qubit processor are, therefore, better suited than other two-qubit gates to compute molecular eigenstates [8, 28]. In fact, using only excitation-preserving gates constrains the accessible state space to a subspace of the full 2^N-dimensional Hilbert space: only the $\binom{N}{n_e}$-dimensional manifold with n_e electrons is explored in VQE, which simplifies the construction of a reduced molecular Hamiltonian [7] and the expansion of the trial wavefunction [8].

In this paper, we show an efficient and scalable approach to compute the energy spectrum of molecules using excitation-preserving exchange-type two-qubit gates.

We demonstrate in simulation that the circuit depth required to achieve chemical accuracy in a VQE algorithms can be significantly reduced by using exchange-type gates, which would allow the simulation of larger quantum systems on near-term quantum hardware. We implement such an exchange-type gate based VQE algorithm on a hardware platform consisting of two fixed-frequency superconducting qubits coupled via a tunable coupler [29, 30] and determine the ground state energy of molecular hydrogen. Finally, we efficiently derive the excited states of molecular hydrogen from the measured ground state using the equation-of-motion (EOM) approach [31], which complements the quantum subspace expansion (QSE) in [25, 32].

II. GATE EFFICIENT QUANTUM CIRCUITS

In quantum chemistry, the molecular Hamiltonian is represented in second quantization [7, 11] as a sum of one and two-body terms and then mapped to the qubit space using a fermion-to-qubit transformation, like the Jordan-Wigner [26] or the parity mapping transformation [33]. Suitable trial states for VQE can be computed with a unitary coupled cluster (UCC) ansatz [34], which is however costly in terms of quantum gates [7, 8]. Alternatively, trial states are generated heuristically by a parametrized sequence of gates directly available in hardware [8]. In the original formulation [24], the heuristic trial wavefunction was generated in the full Fock-space, thus including states with all possible numbers of electrons. With each qubit being mapped to the population of an electronic orbital this corresponds to a Hilbert space spanned by the 2^N basis states $\{i_1, i_2, ..., i_N\}$ with $i_k = 0, 1$. However, if the solution of interest lies in the sector of the Hilbert space with a well-defined number of electrons n_e, i.e. when $\sum_k i_k = n_e$, it is advantageous to use gates that conserve the total number of excitations over the entire qubit register for the trial state preparation.

The simplest method is to prepare the initial state with n_e qubit exciations e.g. $|1_1, 1_2, ..., 1_{n_e}, 0, ..., 0\rangle$ and apply only gates $(\hat{\sigma}^+ + \hat{\sigma}^- + h.c.)$ that exchange excitations between qubits by creating $(\hat{\sigma}^+)$ and annihilating $(\hat{\sigma}^-)$ excitations at the same time. The size of the restricted subspace is then given by $\binom{N}{n_e} \leq 2^N$. Close to half-filling with $n_e \approx N/2$, the advantage is small since $\binom{N}{n_e} \approx 2^{N/2}$. For many molecules however, the number of electrons is typically $n_e \approx N/10$ [35] and the size of the restricted subspace $\binom{N}{n_e} \approx (N/n_e)^{n_e}$ is significantly smaller than that of the full Hilbert space. We note that the restriction of the search space to a given number of electrons prevents the VQE from getting trapped in local minima with an unphysical number of electrons, which is beneficial in particular for multi-electron systems.

In a VQE simulation, the size of the explored subspace is directly connected to the circuit depth required to reach a certain accuracy. Assuming error free gates and using the minimal basis set of atomic orbitals typically used in quantum chemistry [36], we estimate the circuit depth required to achieve chemical accuracy in a VQE simulation of the molecules H_2, LiH, BeH_2 and H_2O (see Fig.1) [37]. Heuristic non excitation-conserving circuits, based e.g. on CNOT gates [24, 38], can in principle achieve chemical accuracy for these molecules. However, the required circuit depth becomes prohibitively large for molecules bigger than H_2 as the circuit runtime exceeds the best relaxation times $T_1 \sim 100\ \mu$s currently available in superconducting hardware. On the other hand, circuits based on excitation-conserving exchange-type gates require a much shorter circuit depth and achieve chemical accuracy for all studied cases within the T_1 limit without further amendments (Fig.1). Clearly, the wanted excitation-preserving two-qubit gate could be decomposed into the available universal gate set [39, 40], e.g. using CNOT gates. But this comes at the expense of an at least tenfold increase in circuit depth (Fig.1) that can be avoided by using application specific hardware and gates. We note that additional reduction schemes can be used to minimize the number of qubits as demonstrated in Ref. [24] for H_2, LiH, BeH_2 and as discussed in the following for the proof-of-principle determination of the eigenspectrum of H_2.

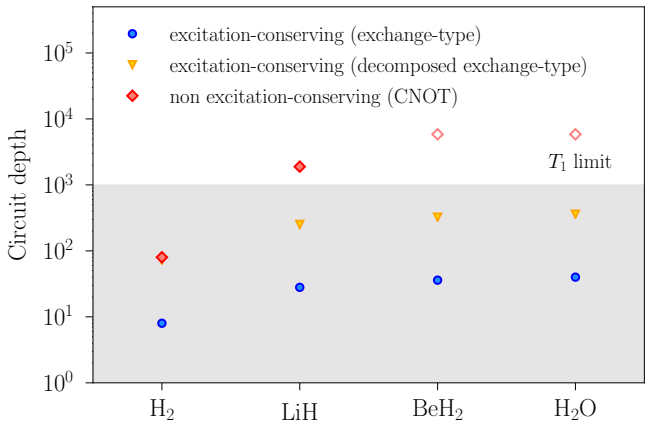

Figure 1. Circuit depth required to achieve chemical accuracy for the ground state energy with a VQE algorithm for the H_2, LiH, BeH_2 and H_2O molecules. Non excitation-conserving circuits based on CNOT gates (red squares) are compared to excitation-conserving circuits based on exchange-type gates (blue circles) and a decomposition thereof into CNOT's (yellow triangles). In some cases, only a lower boundary to the circuit depth could be estimated (empty symbols). Bounded by the T_1 time in the currently available hardware, only circuits within the grey region can be practically implemented without error mitigation or reduction schemes (see text).

III. EXCHANGE TYPE GATES IN A TUNABLE COUPLER ARCHITECTURE

An exchange-type gate primitive can naturally be realized in a tunable coupler architecture (Fig. 2) [29, 30, 41].

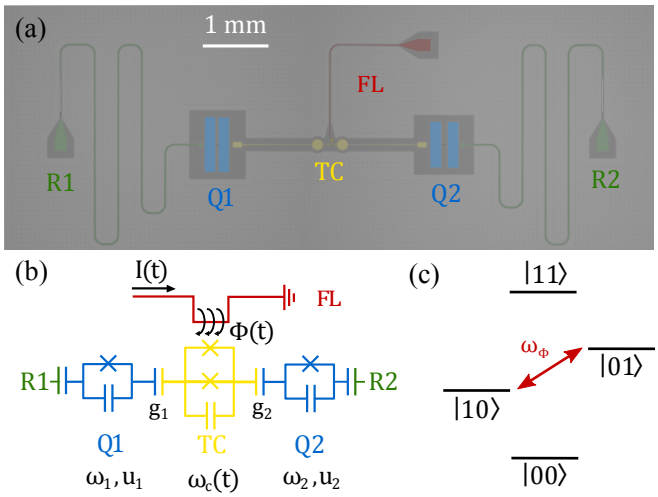

Figure 2. (a) Optical micrograph and (b) circuit scheme of the device consisting of two fixed-frequency transmons (Q1, Q2) capacitatively coupled to a flux-tunable transmon acting as tunable coupler (TC). The tunable coupler is controlled by a flux line (FL) providing a current $I(t)$ and a consequent flux $\Phi(t) = \Phi_{DC} + \delta\cos(\omega_\Phi t + \varphi_\Phi)$ threading the SQUID-loop of the coupler. Each of the fixed-frequency qubits is coupled to an individual readout resonator (R1, R2). (c) Level diagram of the device. Here, $|n_1 n_2\rangle$ denotes the state of the combined system with the qubit excitation number $n_{1,2}$. Modulation of the magnetic flux $\Phi(t)$ at the qubits difference frequency $\omega_\Phi = \omega_1 - \omega_2$ drives the transition between $|10\rangle$ and $|01\rangle$.

The device consists of two fixed-frequency transmon qubits Q1 and Q2 linked via a tunable coupler (TC), i.e. a frequency-tunable transmon [37]. An exchange-type coupling between the computational qubits Q1 and Q2 is achieved by parametric modulation of the TC frequency $\omega_c(t) = \omega_c^0\sqrt{|\cos(\pi\Phi(t)/\Phi_0)|}$ [29, 30]. Threading a magnetic flux $\Phi(t) = \Phi_{DC} + \delta\cos(\omega_\Phi t + \varphi_\Phi)$ with $\omega_\Phi = \omega_1 - \omega_2$ through the SQUID loop of the TC implements the effective Hamiltonian [30]

$$\hat{H}_{\text{eff}} = -\frac{\Omega_{\text{eff}}}{4}\left[\cos\varphi\,(XX+YY) - \sin\varphi\,(YX-XY)\right] \quad (1)$$

with the set of Pauli operators $\{X, Y, Z\} \equiv \{\hat{\sigma}_x, \hat{\sigma}_y, \hat{\sigma}_z\}$. It describes an exchange-type interaction between $|10\rangle$ and $|01\rangle$ at a rate $\Omega_{\text{eff}}(\Phi_{DC}, \delta)$ (Fig. 2(c)). In the following, $\Phi_{DC} = 0.195\Phi_0$ if not stated otherwise. The resulting two-qubit gate operation is described by the unitary operator

$$\hat{U}_{\text{EX}}(\theta,\varphi) = \begin{pmatrix} 1 & 0 & 0 & 0 \\ 0 & \cos\theta/2 & ie^{i\varphi}\sin\theta/2 & 0 \\ 0 & ie^{-i\varphi}\sin\theta/2 & \cos\theta/2 & 0 \\ 0 & 0 & 0 & 1 \end{pmatrix} \quad (2)$$

Here, $\theta = \Omega_{\text{eff}}\tau = \pi\tau/\tau_\pi$ is controlled by the length τ of the tunable coupler drive pulse and $\tau_\pi = 170$ ns is the length of an iSWAP gate, which completely transfers an excitation from one qubit to the other. The phase $\varphi = \varphi_\Phi$ is controlled by the phase φ_Φ of the tunable coupler drive.

To benchmark the efficiency of the exchange-type gate primitive, we perform quantum process tomography (QPT) of $\hat{U}_{\text{EX}}$ as function of φ for a fixed $\theta = \pi$. The overlap of the measured process matrix $\chi_{\text{meas}}(\varphi)$ with an ideal process matrix χ_{ideal} yields the gate fidelity $\mathcal{F} = \text{Tr}(\chi_{\text{meas}}(\varphi)\chi_{\text{ideal}})$. If the measured process matrices are compared with the ideal process matrix of a $\hat{U}_{\text{EX}}(\pi,\varphi)$ operation, the gate fidelity is constant over φ with an average of $\mathcal{F} = 94.2 \pm 1.5\%$ [Fig. 3(a)]. However, if the measured process matrices are compared with the ideal process matrix of $\hat{U}_{\text{EX}}(\pi, 0)$, equivalent to an iSWAP gate operation, the gate fidelity is phase dependant. A fit with the analytic expression

$$\mathcal{F}_{\text{ana}} = \mathcal{F}_0|e^{-2i(\varphi-\varphi_0)}(1+e^{i(\varphi-\varphi_0)})^4| \quad (3)$$

yields a maximum gate fidelity of $\mathcal{F}_0 = 93.2 \pm 0.5\%$ achieved for $\varphi_0 = 3 \pm 5$ mrad (Fig. 3(a)). Similarly, a comparison with the ideal process matrix of $\hat{U}_{\text{EX}}(\pi, \pi/2)$ and $\hat{U}_{\text{EX}}(\pi,\pi)$ yields a maximum gate fidelity at $\varphi_0 = 1.574 \pm 0.007$ rad and $\varphi_0 = 3.155 \pm 0.006$ rad, respectively. It should be noted that the gate fidelity estimation via QPT is subject to state preparation and measurement (SPAM) errors. Other techniques like randomized benchmarking are robust against such SPAM errors, but are mostly limited to gates from the Clifford group. For an iSWAP as a two-qubit gate primitive, we find an error per gate of 3.7% via randomized benchmarking [37].

Furthermore, we perform QPT of $\hat{U}_{\text{EX}}$ as function of θ, i.e. for different lengths τ of the drive pulse on the tunable coupler. Comparing the measured process matrices with the ideal process matrix of $\hat{U}_{\text{EX}}(\theta, \varphi_{\text{opt}})$ yields gate fidelities ranging from $\mathcal{F} = 96 \pm 2.5\%$ (for small θ) to $\mathcal{F} = 91 \pm 1.5\%$ (for large θ) (Fig. 3(b)). Here, the phase φ_{opt} is calibrated to maximize fidelity. The observed decrease of gate fidelity with increasing θ, i.e. longer pulse length τ, can be fitted to an exponential function with a decay time of 6.7 μs, close to the measured relaxation time $T_1 = 6.3$ μs of the TC.

IV. COMPUTATION OF MOLECULAR ENERGY SPECTRA

To demonstrate the usefulness of this gate, we now compute the ground state and the three excited states of molecular hydrogen. Using a parity mapping transformation [33], we map the fermionic second-quantized Hamiltonian of molecular hydrogen to the two-qubit Hamiltonian

$$\hat{H}_{\text{H}_2} = \alpha_0 II + \alpha_1 ZI + \alpha_2 IZ + \alpha_3 ZZ + \alpha_4 XX \quad (4)$$

where α_i denote pre-factors that are classically computed as a function of the bond length of the molecule in the STO-3G basis [42] using PyQuante [37, 43].

To compute the ground state at a given bond length, we use a VQE algorithm as described in [24]. In our case, the respective trial states are of the

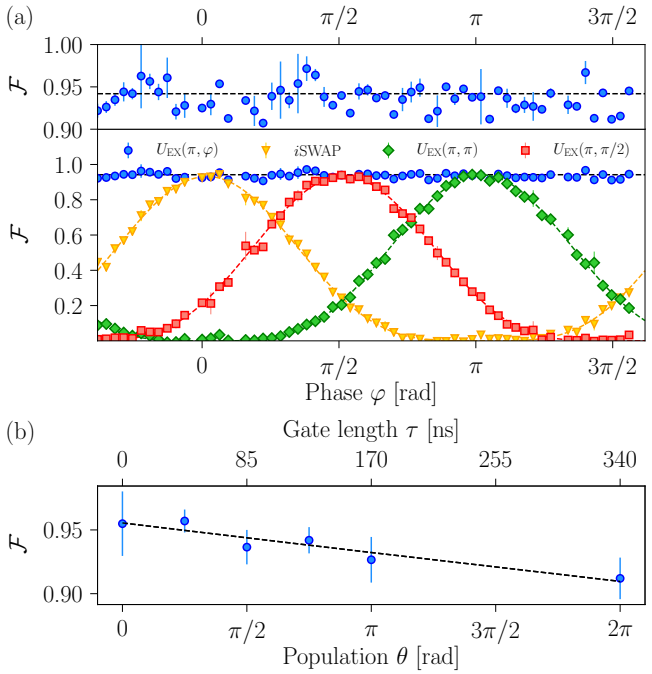

Figure 3. Quantum process tomography of the chemistry gate $\hat{U}_{\mathrm{EX}}(\theta,\varphi)$. (a) Gate fidelities $\mathcal{F}$ as a function of φ for $\theta=\pi$. The bottom panel shows the gate fidelities calculated from the overlap of the measured process matrices $\chi_{\mathrm{meas}}(\varphi)$ with the ideal process matrix χ_{ideal} of a $\hat{U}_{\mathrm{EX}}(\pi,\varphi)$ (blue dots), iSWAP (orange triangles), $\hat{U}_{\mathrm{EX}}(\pi,\pi/2)$ (red squares) and $\hat{U}_{\mathrm{EX}}(\pi,\pi)$ (green diamonds) gate operation. The top panel shows the gate fidelities with respect to $\hat{U}_{\mathrm{EX}}(\pi,\varphi)$. Black dashed lines depicts the average gate fidelity for $\hat{U}_{\mathrm{EX}}(\pi,\varphi)$ (see text). Colored dashed lines are a fit to equation 3. (b) Gate fidelities $\mathcal{F}$ as a function of θ where the phase φ_{opt} is tuned to maximize QPT fidelity. Dashed line is a fit with an exponential decay function with a decay time of 6.7 μs.

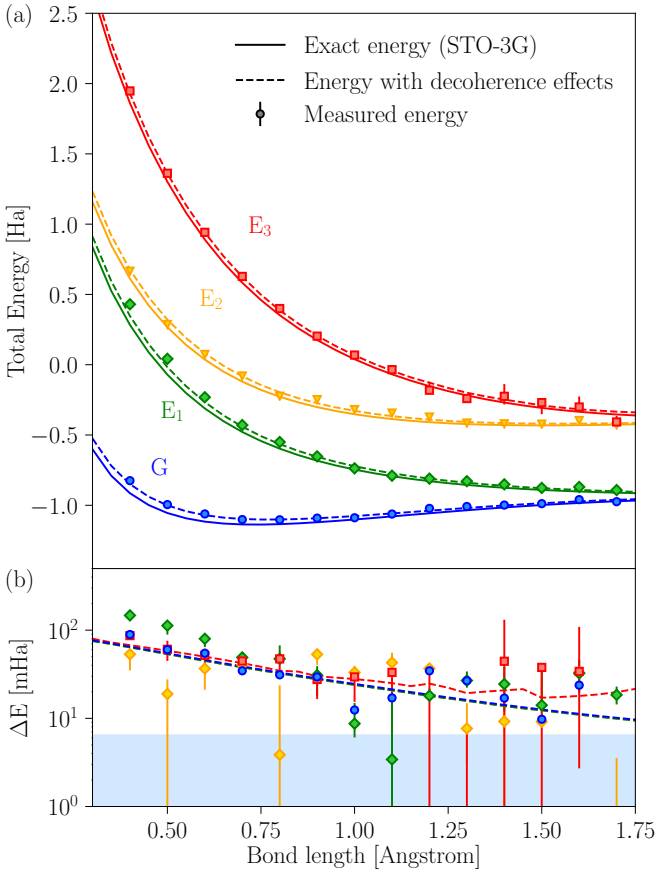

Figure 4. Experimental VQE solution for the ground state and EOM solution for the excited states of molecular hydrogen using a tunable coupling architecture. (a) Ground (G) and excited state (E_1, E_2, E_3) energies as function of bond length. The symbols depict the experimental VQE solution, the solid lines represent the exact solution from the diagonalization of $\hat{H}_{\mathrm{H_2}}$, the dashed line represent the solution including decoherence effects. (b) Accuracy for ground and excited state energies as function of bond length. The symbols correspond to the accuracy of the measured ground and excited state energy determined with respect to the exact solution, while the dashed lines correspond to the expected accuracy including decoherence effects (see text). The depicted ground (excited) state energy is the minimum (median) value from a set of 5 measurements. The errorbars depict the range between the 1st and 3rd quantile (excited states only). The blue shaded area represents the region of chemical accuracy from 0 to 6.5 mHa.

form $|\psi(\theta,\varphi)\rangle = a(\theta,\varphi)\,|01\rangle + b(\theta,\varphi)\,|10\rangle$ and can be realized in a single step with the exchange-type gate primitive $\hat{U}_{\mathrm{EX}}(\theta,\varphi)$. A simultaneous pertubation stochastic approximation (SPSA) algorithm [44] then searches for a state $|\psi(\vec{\theta}_{\mathrm{opt}})\rangle = |\psi(\theta_{\mathrm{opt}},\varphi_{\mathrm{opt}})\rangle$ that minimizes the energy of the molecule $E(\theta_{\mathrm{opt}},\varphi_{\mathrm{opt}}) = \langle\psi(\theta_{\mathrm{opt}},\varphi_{\mathrm{opt}})|\hat{H}_{\mathrm{H_2}}|\psi(\theta_{\mathrm{opt}},\varphi_{\mathrm{opt}})\rangle$ for a given bond length [37]. By changing the parameters α_i in Eq. 4 and running the VQE again for the modified Hamiltonian, we compute the ground state energy of molecular hydrogen as a function of the bond length (Fig. 4).

Furthermore, we compute the excited states of molecular hydrogen following the equation of motion (EOM) approach [37]. Using a variational method, we obtain a pseudo-eigenvalue system of equations which describes the excitations of the system. The matrix elements of this pseudo-eigenvalue system correspond to expectation values of a modified Hamiltonian with the ground state. For each bond length, we measure these matrix elements using the ground state $|\psi(\theta_{\mathrm{opt}},\varphi_{\mathrm{opt}})\rangle$ computed previously with VQE and solve the pseudo-eigenvalue system classically. The solution of this eigenvalue problem then yields the excited state energies. For each bond length, we perform five runs of the experiment and plot the minimum value for the ground state energy and the median value for all excited state energies (symbols in Fig 4(a)). Comparing this experimental solution with the exact solution from a diagonalization of the Hamiltonian $\hat{H}_{\mathrm{H_2}}$ yields the accuracy ΔE (symbols in Fig. 4(b)).

For both ground and excited states, ΔE decreases with the bond length while staying above chemical ac-

curacy (defined here by 6.5 mHa as in [8]). In order to understand this behavior, we study the influence of decoherence effects on the accuracy. Using the decoherence rates and solving a Lindblad-type master equation via QuTIP [37, 45], we obtain ground and excited state energies which now deviate from the exact solution due to decoherence effects (dashed lines in Fig. 4(a) and (b)). The numerical simulations are in good agreement with the experimental data indicating that decoherence has a strong influence on the measured accuracy in our experiment. In particular, the short coherence time $T^*_{2,\mathrm{TC}} = 20$ ns of the tunable coupler in the present hardware is identified as the main cause of inaccuracy. Our simulations indicate that tunable couplers with coherence times of $T^*_{2,TC} > 500$ ns would enable us to reach chemical accuracy and gate fidelities of $\mathcal{F}_{\mathrm{EX}} > 98.9\%$ for an exchange-type gate in the present architecture, which exhibits a ZZ crosstalk between qubit of $\zeta = (\omega_{|11\rangle} - \omega_{|10\rangle} - \omega_{|01\rangle} + \omega_{|00\rangle})/2\pi = -144$ kHz [37]. We note that errors in the optimization and measurement of the ground state $|\psi(\theta_{\mathrm{opt}}, \varphi_{\mathrm{opt}})\rangle$ can induce additional errors in the excited state energies. For comparison, we evaluate ground and excited state energies using the QSE method described in [25, 32]. Due to the linear response expansion in the qubit space, additional spurious states appear in the molecular spectrum and a larger spread in the measured accuracies is observed for the QSE method [37]. In contrast, no spurious states appear in EOM calculations and the accuracy spread is reduced. A detailed analysis of the different errors affecting the excited state calculation is beyond the scope of this work and will be discussed elsewhere [46].

Furthermore, we evaluate the scalability of our computational methods to larger molecular systems. Using the Qiskit Aqua package [47], we estimate the number of Pauli strings $\langle \hat{O}_1 ... \hat{O}_N \rangle$ ($\hat{O} = \{I, X, Y, Z\}$ and N the number of qubits) required to calculate the ground and excited state energies to be $\mathcal{O}(N^4)$ and $\mathcal{O}(N^8)$ respectively, i.e a polynomial increase in the number of measurements [46]. As for the hardware components we note that the tunable coupler elements can be regarded as transmon-type qubits with demonstrated scalability up to 20 qubits [20, 22, 48] and future systems approaching 100 qubits. In such architectures, larger molecules like water could be computed. Since the circuit depth of algorithms based on exchange-type gate is shorter than ones based on CNOT gates, gate errors can be up to an order of magnitude higher to reach chemical accuracy [37].

V. CONCLUSION

In conclusion, we demonstrate a gate-efficient way to simulate molecular spectra on a tailor-made superconducting qubit processor using exchange-type two-qubit gates. With the choice of excitation-preserving exchange-type gates, tunable in both amplitude and phase, we preserve the number of excitations in the system and achieve the reduction of the VQE entangler to a single gate primitive. This enables the efficient computation of the molecular ground state, which can subsequently be used to efficiently calculate the molecule's excited states using an EOM approach. In the present case, the accuracy of the computation is still limited by the coherence time of the tunable coupling element. However, error mitigation schemes [49, 50] or minor improvements to the coherence of the coupler would allow us to reach chemical accuracy. Our findings show that adapting quantum algorithms and hardware to the problem at hand is a key requirement to perform quantum simulation on a larger scale. In particular, exchange-type gates are a promising choice to compute the energy spectra of larger molecules like water on near-term quantum hardware.

ACKNOWLEDGMENTS

We thank the quantum team at IBM T. J. Watson Research Center, Yorktown Heights, in particular the fab team, Jerry Chow, David McKay and William Shanks for insightful discussions and the provision of qubit devices. We thank R. Heller and H. Steinauer for technical support. We thank S. Hoenl for designing a teaser image for this article. This work was supported by the IARPA LogiQ program under contract W911NF-16-1-0114-FE and the ARO under contract W911NF-14-1-0124.

[1] Richard P. Feynman, "Simulating physics with computers," Int. J. Theor. Phys. **21**, 467–488 (1982).
[2] Ryan Babbush, Peter J. Love, and A. Aspuru-Guzik, "Adiabatic quantum simulation of quantum chemistry," Scientific Reports **4**, 6603– (2014).
[3] Alexey Yu. Kitaev, "Quantum measurement and the abelian stabilizer problem," arXiv.9511026v1 (1995).
[4] Dave Wecker, Bela Bauer, Bryan K. Clark, Matthew B. Hastings, and Matthias Troyer, "Gate-count estimates for performing quantum chemistry on small quantum computers," Phys. Rev. A **90**, 022305 (2014).
[5] Austin G. Fowler, Matteo Mariantoni, John M. Martinis, and Andrew N. Cleland, "Surface codes: Towards practical large-scale quantum computation," Phys. Rev. A **86**, 032324 (2012).
[6] Alberto Peruzzo, Jarrod McClean, Peter Shadbolt, Man-Hong Yung, Xiao-Qi Zhou, Peter J. Love, A. Aspuru-Guzik, and Jeremy L. O'Brien, "A variational eigenvalue solver on a photonic quantum processor," Nature Communications **5**, 4213– (2014).

[7] Nikolaj Moll, Panagiotis Barkoutsos, Lev S. Bishop, Jerry M. Chow, Andrew Cross, Daniel J. Egger, Stefan Filipp, Andreas Fuhrer, Jay M. Gambetta, Marc Ganzhorn, Abhinav Kandala, Antonio Mezzacapo, Peter Müller, Walter Riess, Gian Salis, John Smolin, Ivano Tavernelli, and Kristan Temme, "Quantum optimization using variational algorithms on near-term quantum devices," Quantum Science and Technology **3**, 030503 (2018).

[8] Panagiotis Kl. Barkoutsos, Jerome F. Gonthier, Igor Sokolov, Nikolaj Moll, Gian Salis, Andreas Fuhrer, Marc Ganzhorn, Daniel J. Egger, Matthias Troyer, Antonio Mezzacapo, Stefan Filipp, and Ivano Tavernelli, "Quantum algorithms for electronic structure calculations: Particle-hole hamiltonian and optimized wavefunction expansions," Phys. Rev. A **98**, 022322 (2018).

[9] Ian D. Kivlichan, Jarrod McClean, Nathan Wiebe, Craig Gidney, Alan Aspuru-Guzik, Garnet Kin-Lic Chan, and Ryan Babbush, "Quantum simulation of electronic structure with linear depth and connectivity," Phys. Rev. Letts. **120**, 110501 (2018).

[10] Jarrod R. McClean, Jonathan Romero, Ryan Babbush, and Alan Aspuru-Guzik, "The theory of variational hybrid quantum-classical algorithms," New Journal of Physics **18**, 023023 (2016).

[11] Ryan Babbush, Nathan Wiebe, Jarrod McClean, James McClain, Hartmut Neven, and Kin-Lic Garnet Chan, "Low depth quantum simulation of electronic structure," Phys. Rev. X **8**, 011044 (2018).

[12] Benjamin P Lanyon, James D. Whitfield, Geoff G. Gillett, Michael E. Goggin, Marcelo P. Almeida, Ivan Kassal, Jacob D. Biamonte, Masoud Mohseni, Ben J. Powell, Marco Barbieri, Alan Aspuru-Guzik, and Andrew G. White, "Towards quantum chemistry on a quantum computer," Nat Chem **2**, 106–111 (2010).

[13] Jiangfeng Du, Nanyang Xu, Xinhua Peng, Pengfei Wang, Sanfeng Wu, and Dawei Lu, "NMR implementation of a molecular hydrogen quantum simulation with adiabatic state preparation," Phys. Rev. Lett. **104**, 030502 (2010).

[14] Bei-Bei Li, Yun-Feng Xiao, Chang-Ling Zou, Yong-Chun Liu, Xue-Feng Jiang, You-Ling Chen, Yan Li, and Qihuang Gong, "Experimental observation of fano resonance in a single whispering-gallery microresonator," Appl. Phys. Lett. **98**, 021116 (2011).

[15] Chen Wang, Christopher Axline, Yvonne Gao, Teresa Brecht, Yiwen Chu, Luigi Frunzio, Michel Devoret, and Robert Schoelkopf, "Surface participation and dielectric loss in superconducting qubits," Appl. Phys. Lett. **107**, 162601 (2015).

[16] Christopher Monroe and Jungsang Kim, "Scaling the ion trap quantum processor," Science **339**, 1164 (2013).

[17] Jiehang Zhang, Guido Pagano, Paul W. Hess, Antonis Kyprianidis, Patrick Becker, Harvey Kaplan, Alexey V. Gorshkov, Z.X. Gong, and Christopher Monroe, "Observation of a many-body dynamical phase transition with a 53-qubit quantum simulator," Nature **551**, 601–604 (2017).

[18] Hannes Bernien, Sylvain Schwartz, Alexander Keesling, Harry Levine, Ahmed Omran, Hannes Pichler, Soonwon Choi, Alexander S. Zibrov, Manuel Endres, Markus Greiner, Vladan Vuletic, and Mikhail D. Lukin, "Probing many-body dynamics on a 51-atom quantum simulator," Nature **551**, 579–584 (2017).

[19] Cornelius Hempel, Christine Maier, Jonathan Romero, Jarrod McClean, Thomas Monz, Heng Shen, Petar Jurcevic, Ben P. Lanyon, Peter Love, Ryan Babbush, Alán Aspuru-Guzik, Rainer Blatt, and Christian F. Roos, "Quantum chemistry calculations on a trapped-ion quantum simulator," Phys. Rev. X **8**, 031022 (2018).

[20] Charles Neill, Pedram Roushan, K. Kechedhzi, Sergio Boixo, Sergei V. Isakov, Vadim Smelyanskiy, Rami Barends, Brian Burkett, Yu Chen, Zijun Chen, Benjamin Chiaro, Andrew Dunsworth, Austin Fowler, Brooks Foxen, Rob Graff, Evan Jeffrey, Julian Kelly, Erik Lucero, A. Megrant, Josh Y. Mutus, Matthew Neeley, Chris Quintana, Daniel Sank, Amit Vainsencher, Jim Wenner, Ted C. White, Hartmut Neven, and John M. Martinis, "A blueprint for demonstrating quantum supremacy with superconducting qubits," Science **360**, 195–199 (2018).

[21] Johannes S. Otterbach, Ricardo Manenti, Nasser Alidoust, Andrew Bestwick, Maxwell Block, Benjamin Bloom, Shane Caldwell, Nicolas Didier, E. Schuyler Fried, Sabrina Hong, P. Karalekas, Christopher B. Osborn, Alexander Papageorge, E. C. Peterson, G. Prawiroatmodjo, Nicholas Rubin, Colm A. Ryan, Diego Scarabelli, Michael Scheer, Eyob A. Sete, Prasahnt Sivarajah, R. S. Smith, A. Staley, Nikolas Tezak, William J. Zeng, A. Hudson, Blake R. Johnson, Matthew Reagor, Marcus P. da Silva, and Chad Rigetti, "Unsupervised machine learning on a hybrid quantum computer," arXiv:1712.05771 (2017).

[22] International Business Machines Corporation, "IBM Q Experience," (2016).

[23] Peter J. J. O'Malley, Ryan Babbush, Ian D. Kivlichan, Jonathan Romero, Jarod R. McClean, Rami Barends, Julian Kelly, Pedram Roushan, Andrew Tranter, Nan Ding, B. Campbell, Yiwen Chen, Zijun Chen, Benjamin Chiaro, Andrew Dunsworth, Austin G. Fowler, Evan Jeffrey, Erik Lucero, Anthony Megrant, Josh Y. Mutus, Matthew Neeley, Charles Neill, Chris Quintana, Daniel Sank, Amit Vainsencher, Jim Wenner, Ted C. White, Peter V. Coveney, Peter J. Love, Hartmut Neven, Alan Aspuru-Guzik, and John M. Martinis, "Scalable quantum simulation of molecular energies," Phys. Rev. X **6**, 031007 (2016).

[24] Abhinav Kandala, Antonio Mezzacapo, Kristan Temme, Maika Takita, Markus Brink, Jerry M. Chow, and Jay M. Gambetta, "Hardware-efficient quantum optimizer for small molecules and quantum magnets," Nature **549**, 242–246 (2017).

[25] James I. Colless, Vinay V. Ramasesh, Dar Dahlen, Machiel S. Blok, Jarrod R. McClean, Jonathan Carter, Wibe A. de Jong, and Irfan Siddiqi, "Robust determination of molecular spectra on a quantum processor," Phys. Rev. X **8**, 011021 (2018).

[26] Pascual Jordan and Eugene Wigner, "über das Paulische äquivalenzverbot," Zeitschrift für Physik **47**, 631 (1928).

[27] Sergey B. Bravyi and Alexei Yu. Kitaev, "Fermionic quantum computation," Annals of Physics **298**, 210 – 226 (2002).

[28] Felix Motzoi, Michael P. Kaicher, and Frank K. Wilhelm, "Linear and logarithmic time compositions of many-body systems," Phys. Rev. Lett. **119**, 160503 (2017).

[29] David C. McKay, Stefan Filipp, Antonio Mezzacapo, Easwar Magesan, Jerry M. Chow, and Jay M. Gambetta, "Universal gate for fixed-frequency qubits via a

tunable bus," Phys. Rev. Applied **6**, 064007 (2016).
[30] Marco Roth, Marc Ganzhorn, Nikolaj Moll, Stefan Filipp, Gian Salis, and Sebastian Schmidt, "Analysis of a parametrically driven exchange-type gate and a two-photon excitation gate between superconducting qubits," Phys. Rev. A **96**, 062323 (2017).
[31] D.J. Rowe, "Equations-of-motion method and the extended shell modell," Rev. Mod. Phys **40**, 153 (1968).
[32] Jarrod R. McClean, Mollie E. Kimchi-Schwartz, Jonathan Carter, and Wibe A. de Jong, "Hybrid quantum-classical hierarchy for mitigation of decoherence and determination of excited states," Phys. Rev. A **95**, 042308 (2017).
[33] Sergey Bravyi, Jay M. Gambetta, Antonio Mezzacapo, and Kristan Temme, "Tapering off qubits to simulate fermionic hamiltonians," arXiv:1701.08213 (2017).
[34] Andrew G. Taube and Rodney J. Bartlett, "New perspectives on unitary coupled cluster theory," Int. J. Quantum Chem. , 3393–3401 (2006).
[35] National Institute of Science and Technology, "Computational Chemistry Comparison and Benchmark Database," (2018).
[36] John A. Pople and David L. Beveridge, *Approximate molecular orbital theory* (McGraw-Hill book company, 1970).
[37] "See supplemental material at [url filed in by editor] for additional information,".
[38] Sarah Sheldon, Easwar Magesan, Jerry M. Chow, and Jay M. Gambetta, "Procedure for systematically tuning up cross-talk in the cross-resonance gate," Phys. Rev. A **93**, 060302 (2016).
[39] Adriano Barenco, Charles H. Bennett, Richard Cleve, David P. DiVincenzo, Norman Margolus, Peter Shor, Tycho Sleator, John A. Smolin, and Harald Weinfurter, "Elementary gates for quantum computation," Phys. Rev. A **52**, 3457–3467 (1995).
[40] Michael A. Nielsen and Isaac L. Chuang, *Quantum Computation and Quantum Information* (Cambridge University Press, 2000).
[41] Yu Chen, Charles Neill, Pedram Roushan, Nelson Leung, Ming Fang, Rami Barends, Julian Kelly, B. Campbell, Zijun Chen, Benjamin Chiaro, Andrew Dunsworth, Evan Jeffrey, Anthony Megrant, Josh Y. Mutus, Peter J. J. O'Malley, Chris M. Quintana, Daniel Sank, Amit Vainsencher, Jim Wenner, Ted C. White, M. R. Geller, Andrew N. Cleland, and John M. Martinis, "Qubit architecture with high coherence and fast tunable coupling," Phys. Rev. Letts. **113**, 220502 (2014).
[42] Warren J. Hehre, Robert Ditchfield, and John A. Pople, "Self—consistent molecular orbital methods. xii. further extensions of gaussian—type basis sets for use in molecular orbital studies of organic molecules," The Journal of Chemical Physics **56**, 2257–2261 (1972).
[43] Richard P. Muller, "Python quantum chemistry, version 2," .
[44] James C. Spall, "Implementation of the simultaneous perturbation algorithm for stochastic optimization," IEEE Transactions on Aerospace and Electronic Systems **34**, 817–823 (1998).
[45] J. Robert Johansson, Paul D. Nation, and Franco Nori, "Qutip 2: A python framework for the dynamics of open quantum systems," Computer Physics Communications **184**, 1234 – 1240 (2013).
[46] P. Ollitrault and et al, In preparation.
[47] Gadi Aleksandrowicz, Thomas Alexander, Panagiotis Barkoutsos, Luciano Bello, Yael Ben-Haim, David Bucher, Francisco Jose Cabrera-Hernádez, Jorge Carballo-Franquis, Adrian Chen, Chun-Fu Chen, Jerry M. Chow, Antonio D. Córcoles-Gonzales, Abigail J. Cross, Andrew Cross, Juan Cruz-Benito, Chris Culver, Salvador De La Puente González, Enrique De La Torre, Delton Ding, Eugene Dumitrescu, Ivan Duran, Pieter Eendebak, Mark Everitt, Ismael Faro Sertage, Albert Frisch, Andreas Fuhrer, Jay Gambetta, Borja Godoy Gago, Juan Gomez-Mosquera, Donny Greenberg, Ikko Hamamura, Vojtech Havlicek, Joe Hellmers, Łukasz Herok, Hiroshi Horii, Shaohan Hu, Takashi Imamichi, Toshinari Itoko, Ali Javadi-Abhari, Naoki Kanazawa, Anton Karazeev, Kevin Krsulich, Peng Liu, Yang Luh, Yunho Maeng, Manoel Marques, Francisco Jose Martín-Fernández, Douglas T. McClure, David McKay, Srujan Meesala, Antonio Mezzacapo, Nikolaj Moll, Diego Moreda Rodríguez, Giacomo Nannicini, Paul Nation, Pauline Ollitrault, Lee James O'Riordan, Hanhee Paik, Jesús Pérez, Anna Phan, Marco Pistoia, Viktor Prutyanov, Max Reuter, Julia Rice, Abdón Rodríguez Davila, Raymond Harry Putra Rudy, Mingi Ryu, Ninad Sathaye, Chris Schnabel, Eddie Schoute, Kanav Setia, Yunong Shi, Adenilton Silva, Yukio Siraichi, Seyon Sivarajah, John A. Smolin, Mathias Soeken, Hitomi Takahashi, Ivano Tavernelli, Charles Taylor, Pete Taylour, Kenso Trabing, Matthew Treinish, Wes Turner, Desiree Vogt-Lee, Christophe Vuillot, Jonathan A. Wildstrom, Jessica Wilson, Erick Winston, Christopher Wood, Stephen Wood, Stefan Wörner, Ismail Yunus Akhalwaya, and Christa Zoufal, "Qiskit: An open-source framework for quantum computing," (2019).
[48] Sabrina Hong, Alexander T. Papageorge, Pradahnt Sivarajah, Genya Crossman, Nicolas Didier, Anthony Polloreno, Eyob A. Sete, Stefan W. Turkoswki, and Blake R. da Silva, Marcus P. Johnson, "Demonstration of a parametrically-activated entangling gate protected from flux noise," arXiv:1901.08035 (2019).
[49] Kristan Temme, Sergey Bravyi, and Jay M. Gambetta, "Error mitigation for short depth quantum circuits," Phys. Rev. Lett. **119**, 180509 (2017).
[50] Abhinav Kandala, Kristan Temme, Corcoles Antonio D., Antonio Mezzacapo, Jerry M. Chow, and Jay M. Gambetta, "Extending the computational reach of a noisy superconducting quantum processor," arxiv:1805.04492 (2018).